CrystEngComm

Accepted Manuscript

ROYAL SOCIETY OF CHEMISTRY

www.rsc.org/crystengcomm

CrystEngComm RSCPublishing

ARTICLE

Epitaxial growth of self-separation GaN crystals by using a novel high temperature annealing porous template

Cite this: DOI: 10.1039/x0xx00000x

Received 00th January 2012,
Accepted 00th January 2012

DOI: 10.1039/x0xx00000x

www.rsc.org/

Lei Zhang, Yuanbin Dai, Yongzhong Wu, Yongliang Shao, Yuan Tian, Qin Huo, Xiaopeng Hao*, Yinan Shen, Zhen Hua

In this paper, a MOCVD-GaN/Al_2O_3 (MGA) template was annealed with appropriate annealed conditions under N_2 flow to form the porous template. The porous template was used for growing GaN by HVPE. The GaN crystal was easily separated from the porous template by the assistance of the micron-porous structure. The self-separation GaN crystal grown on porous template showed smaller full width at half maximum (FWHM) of (002) and (102) reflections in HRXRD measurement than that grown on MGA template. The PL results indicate that the optical quality of the GaN crystal on the porous template was improved and the dislocation density was decreased. The Raman results showed that the stress of GaN crystal grown on porous template is much smaller than that on MGA template. These results shows that crystalline quality of GaN crystals was improved by using the porous templates.

Introduction

Gallium nitride (GaN) is a wide band gap semiconductor with unique material and electronic properties[1]. It will be widely applied as the key material in manufacturing next generation optoelectronics, high-power and high-frequency devices[2]. GaN provide many advantages for optoelectronic device applications, including high carrier mobility and radiative recombination rates, as well as long-term stability and reliability[3]. By using the soluble salt as the dispersant, a facile synthetic route has been developed to prepare GaN nanoparticles on a large scale and in a high yield (95.8%) through the direct nitridation of Ga-Na_2SO_4 mixtures[4]. The commonly used substrates for growth of thick GaN films are sapphire (Al_2O_3) due to its relatively low price, thermal stability and hexagonal symmetry[5]. However, approximate 14% mismatch in lattice parameters and 19% difference in thermal expansion coefficients between sapphire and GaN lead to high dislocation density and high in-plane strain in GaN[6,7]. The high dislocation density is not conducive to the fabrication of high performance GaN-based devices with long lifetime. To decrease the dislocation density of heteroepitaxial GaN, several techniques have been developed, such as void-assisted separation[8], epitaxial lateral overgrowth (ELOG)[9] and fabrication nanostructure on substrate[10]. The quality of GaN can be improved by using these methods, and correspondingly the dislocation density has been decreased. However, these techniques need complicated growth processes or expensive photolithography.

When GaN is exposed to N_2 flow at temperatures higher than 900 ℃, the compound is decomposed[11,12]. In our previous work, a high temperature annealing method is proposed to determine the pit density with respect to dislocation type and to show their distribution[13]. The decomposition contributes to the morphological reorganization or the corrosion of GaN material under suitable condition[14,15].

Based on this mechanism, we have designed a simple technology to fabricate a novel high temperature annealing porous (HTAP) template. There are few reports on the growth of GaN crystals on a high temperature annealing porous template by hydride vapor phase epitaxy (HVPE). In this study, the fabrication of GaN crystals by HVPE on the HTAP templates and the MGA (MGA is an acronym for MOCVD-GaN/Al_2O_3) template are reported and the surface morphology, structural characteristics and optical properties of the two kinds of GaN crystals are compared.

Experimental

A MOCVD-GaN/Al_2O_3 (MGA) template with a GaN layer of about 5 μm thickness, fabricated by MOCVD on a 2 inch c-plane sapphire substrate, was employed in the subsequent experiments. The MGA templates were grown by Metal-organic Chemical Vapor Deposition (MOCVD) system. Trimethylaluminum (TMAl), trimethylgallium (TMGa) and ammonia (NH_3) were used as precursors, and SiH_4 as the n-type dopant source. The growth pressure was 500 Torr for GaN growth. The growth temperatures were about 1070 °C and 550 °C for GaN and GaN buffer layer, respectively. The thickness of the GaN buffer layer was 25 nm. After the GaN buffer, a 2 μm thick undoped GaN layer was grown on it, followed by a 3 μm thick Si doped GaN layer. The total thickness of GaN epilayer was 5 μm. The MGA template was annealed with appropriate annealed conditions under N_2 flow to form the

State Key Lab of Crystal Materials, Shandong University, Jinan, 250100, PR China. E-mail: xphao@sdu.edu.cn; Fax: +86 53188364864; Tel: +86 53188366218

template with porous structure. By adjusting the annealed temperatures, annealed times and gas flow, the porous GaN with different porosities can be achieved. To incorporate the porous GaN into the proposed self-separation method, we choose the optimal annealed conditions. Then, the HTAP template was mounted in a home-made vertical HVPE reactor to grow GaN crystals. Ga and NH_3 were used as gallium and nitrogen sources. HCl gas reacted with liquid Ga at 820 ℃ to form GaCl, which was transported to the growth zone of the reactor and reacted with NH_3 at 1030 ℃ to form the GaN deposition on the substrate. N_2 was used as the carrier gas. The reactor pressure was kept around atmospheric pressure. The NH_3 flow rate was held in the range 800-1000 mL/min, while the HCl flow rate was 10-20 mL/min. The growth rate was controlled in the range 10-30 μm/h. The thickness of the GaN crystal was about 40 μm.

Scanning electron microscopy (SEM) images were taken with a Hitachi FESEM-4800 field emission microscope equipped
with a Horiba EX-450 energy-dispersive X-ray spectroscopy (EDS). Raman spectra of the samples were obtained by the LabRAM HR system of Horiba Jobin Yvon at room temperature using a 532 nm solid laser as the exciting source. Photoluminescence (PL) measurement was carried out at room temperature using 325 nm He–Cd lasers as excitation power. The crystal quality of the GaN films was characterized by high-resolution X-ray diffraction (HRXRD) using symmetrical (002) and asymmetrical (102) reflections.

Results and discussion

Theoretical foundation and design of the HTAP template

Annealing above a certain temperature can cause GaN decomposition[11,12]. The GaN decomposition reaction has been reported by Boris V. L'vov to be as follows[16]:

$$GaN(s) \rightarrow Ga(g) + (1-i)N + 0.5iN_2 \quad (1)$$

Where the interaction parameter i varies from 0 to 1, depending on the extent to which the nearest nitrogen atoms interact with one another at the instant of decomposition. It is well-known that Ga has the longest temperature range in the liquid phase (from 29.78 to 2403℃)[17]. Therefore, Ga vapor easily turns to liquid in a short time. Liquid Ga may participate as a catalyst in the vaporization process by dissolving Ga and disrupting its rigid wurtzite crystal structure[18]. The critical temperature of the GaN decomposition beginning depended on the annealing conditions (pressure, ambient gas) and the as-grown material properties (surface morphology, film polarity). Jacob et al.[19] measured the decomposition of GaN in different gases and found a value of initial decomposition temperature 970 ℃ in Ar/N_2 and 600℃ in H_2. Rebey et al. found that GaN was stable even when annealed in N_2 at a temperature as high as 1050 ℃ [20]. Bchetnia et al. observed that annealing at temperature above 1100 ℃ causes the decomposition of GaN layers in N_2 atmosphere at atmospheric pressure[21]. In the case of the GaN film with a pre-deposited liquid Ga droplet, noticeable decomposition started after annealing at 720 ℃ for 15min in flowing Ar+H_2 at 1 bar. The surface got rougher and small holes appeared near the Ga-GaN boundary[22]. Microhexagonal pits with average radii of 20 μm were observed on the annealed GaN surface in H_2 atmosphere at 1030℃ for 5 min[15]. After annealing temperature over 1100 ℃ in N_2 atmosphere, the GaN film began to decompose and it had a porous-like surface with a non-uniform distribution of the pore size[21].

Y. Oshima et al. proposed a VAS (void-assisted separation) technique for separating freestanding GaN from sapphire substrates by the assistance of numerous small voids[8]. In the VAS method, a thick GaN layer grown by HVPE was spontaneously separated as a result of thermal stress at a boundary consisting of numerous voids generated around a thin porous TiN layer inserted between the thick GaN layer and the base substrate during the cooling process after the growth freestanding GaN wafers from sapphire substrates by the assistance of numerous small voids. M. G. Mynbaeva et al. reported on the fabrication of porous freestanding GaN substrates using the anodization technique and on the epitaxial growth of GaN films on such substrates[5]. The threading dislocation density was reduced by using the nano-porous structure.

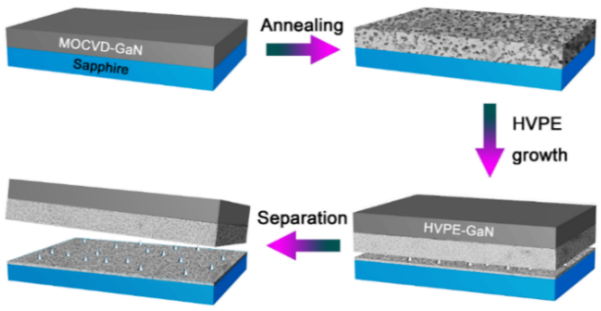

Figure 1. The schematic diagram of GaN crystal grown on the HTAP template.

On the basis of the aforementioned analysis, it can be concluded that the voids or porous structure can block dislocation, release thermal stresses and assist separate GaN from the base substrate. Based on this conclusion, we designed and fabricated the HTAP template. Figure 1 shows the schematic diagram of GaN crystal grown on a HTAP template. A template with a GaN layer of about 5 μm thickness, fabricated by MOCVD on a 2 inch c-plane sapphire substrate, was employed as the starting substrate. The MGA template was annealed at 1100 ℃ for 100 min under N_2 flow (2200 sccm). This annealing process converted the GaN film into a micron-porous structure of GaN. A number of voids were formed in the MOCVD-grown GaN layer. Then, a 40 μm thick GaN crystal was grown on the HTAP template by HVPE. The GaN crystal was easily separated from the HTAP template after taking the sample out of the reactor.

Growth result and discussion

Figure 2(a) shows the surface morphology of the annealed HTAP template. Figure 2(b) shows the cross-section SEM images of the annealed HTAP template. The images show that the MOCVD-GaN layer turned into a micron-porous structure. Some holes easily penetrate through the MOCVD-GaN layer and reach the sapphire substrate. The Al_2O_3 in some holes was confirmed by EDS (Figure 2(c)).

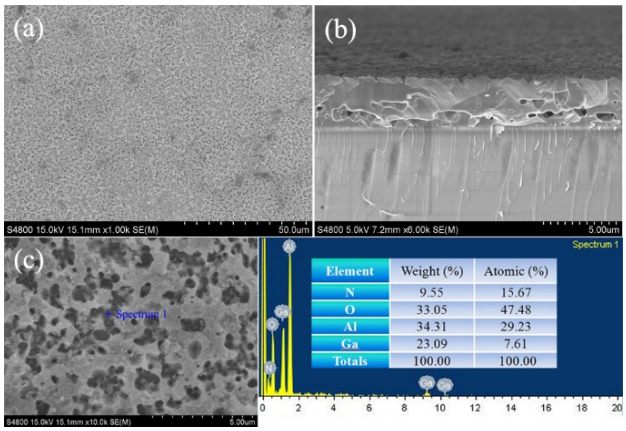

Figure 2(a). SEM image of the surface of the annealed HTAP template. Figure 2(b). Cross-section SEM image of the annealed HTAP template. Figure 2(c). The EDS results of the HTAP template. Spectrum 1 was the EDS result of holes in the HTAP template.

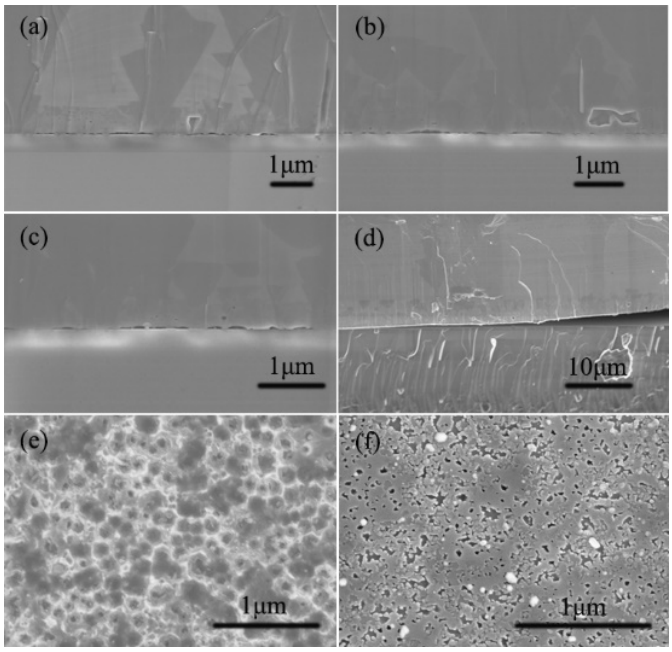

Figure 3(a)-(c) Cross-section SEM image of the GaN crystal grown on the HTAP template. (d) SEM image of GaN crystal separation from the HTAP template. SEM images of (e) the GaN backside and (f) the surface of the base substrate.

Figure 3(a)-(c) show the cross-section SEM images of the GaN crystal grown on the HTAP template. After HVPE-GaN growth, some voids were filled with the coalesced GaN. However, some voids also can be observed between the HVPE grown GaN and sapphire substrate. Figure 3(d) shows the SEM image of GaN crystal separated from the HTAP template. The GaN cyrstal grown on HTAP template was self-separated without any cracks after cooling down. Figure 3 (e)-(f) show the SEM images of the backside of the GaN and the upper surface of the base substrate, respectively. It can be seen that the porous structure remained on the backside of the GaN and the upper surface of the base substrate. This shows that separation occurred at the interface of the thick GaN crystal and the porous, suggesting that the porous structure make an essential contribution to the separation process.

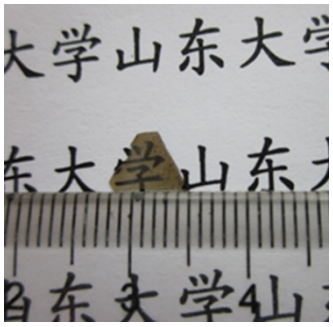

Figure 4. Digital camera image of the lift-off GaN crystal produced using the HTAP template.

Figure 4 shows a digital camera image of the free-standing GaN crystal produced by using the HTAP template. The GaN crystal was completely separated from the sapphire substrate. The size of the GaN crystal could be enlarged if larger templates were used.

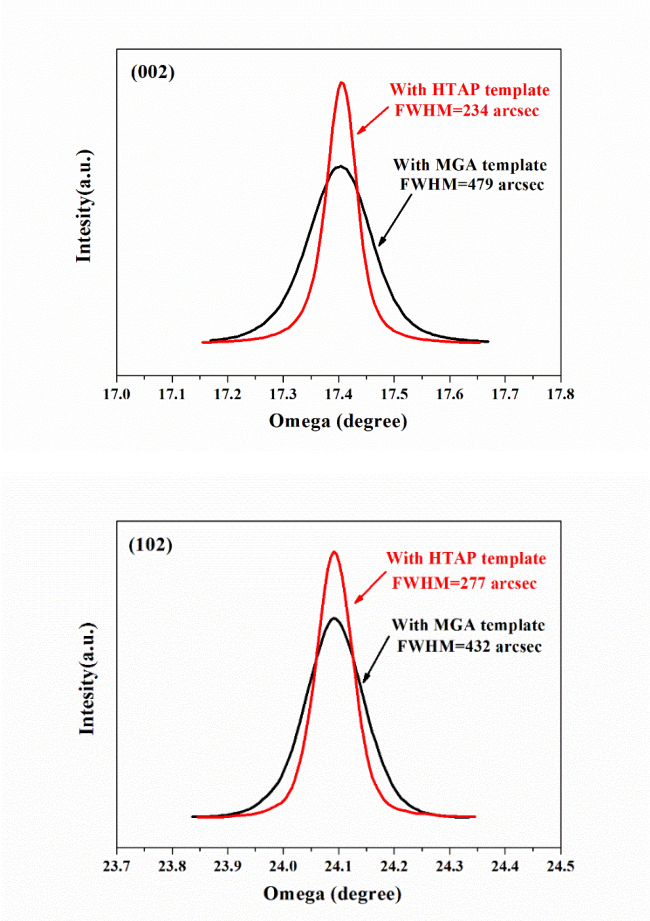

Figure 5. HRXRD rocking curves of HVPE GaN crystals on the HTAP template and the MGA template: (a) (002) ω-scans and (b) (102) ω-scans.

The quality of the self-separation GaN crystals were characterized by HRXRD rocking curves. Figure 5 depicts the ω-scans spectra of (002) symmetry planes and (102) asymmetry planes of the GaN film grown using the HTAP and MGA template. The FWHM of the (002) peak is 234 arcseconds for the GaN crystals grown on the HTAP template and 479 arcseconds for those grown on the MGA template. Meanwhile,

the FWHM of the (102) peak is 277 and 432 arcseconds for the GaN crystals grown on the HTAP and the MGA templates, respectively. It is well known that the FWHM of the HRXRD rocking curve for asymmetrical (102) plane is directly related to the reliability of the structural quality since (102) FWHM is related with all TDs, including pure edge-, screw- and mixed-dislocations[23]. Based on the HRXRD results, it is exhibited that all types of dislocations were reduced by using the HTAP template. The dislocation density ρ can be calculated by the following formula[24]:

$$\rho = \frac{\beta^2}{4.35 \times b^2} \qquad (2)$$

Where β is the absolute value of the Burgers vector and b stands for the FWHM of the rocking curves. The edge dislocation density of GaN on HTAP template is about 4.1×10^8 cm^{-2}, less than the value 9.9×10^8 cm^{-2} in GaN crystal on MGA template, meanwhile screw dislocation density is also reduced from 4.6×10^8 cm^{-2} to 1.1×10^8 cm^{-2}. The calculation result also shows that GaN crystalline quality of our samples was effectively improved by using the HTAP template. The state of the art for dislocation density in free-standing HVPE GaN with thickness of 5.8 mm was 1.2×10^6 cm^{-2}.[25] High quality GaN crystal has dislocation densities an order of magnitude lower than our results (10^7 cm^{-2}). The dislocation density decreased with increase of its thickness [26]. Growth process is also the key factor for growing high quality GaN crystal by HVPE. By prolonging the growth time and adjusting growth process, lower dislocation density GaN crystal grown on HTAP template will be obtained.

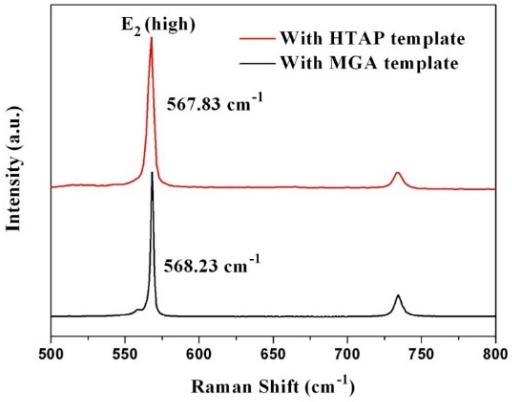

Figure 6. Raman spectra of the GaN crystals grown on the HTAP template and the MGA template.

To measure the strain of GaN crystals, Raman spectra were carried out for both GaN on the MGA and HTAP templates. Figure 6 shows the Raman spectroscopy of GaN crystals. The E_2 phonon mode in the Raman scattering process is known to be sensitive to the biaxial stress in the crystal. The relaxation of residual strain can be measured by the following equation[27]:

$$\sigma = \frac{\Delta\omega}{4.3} \ (\mathrm{cm^{-1}GPa^{-1}}) \qquad (3)$$

where σ is the biaxial stress and Δω is the E_2 phonon peak shift. The E_2 (high) phonon frequency of GaN crystals grown on the HTAP and MGA templates are 567.83 cm and 568.23 cm, respectively. This redshift of 0.4 cm^{-1} corresponds to a relaxation of compressive stress by 0.14 GPa. It demonstrated that the GaN crystal grown on the HTAP template reduced the biaxial stress of epitaxial GaN which could be advantageous for the growth of high quality GaN.

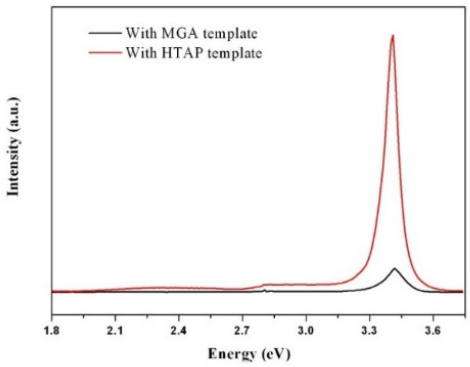

Figure 7 PL spectra of the GaN crystals grown on the MGA template and the HTAP template.

The optical quality of the GaN crystals grown on the HTAP template is further characterized by PL and compared to that of GaN crystal on MGA template (Figure 7). A sharp and strong band edge emission on the MGA and HTAP template is observed. Their emission peaks are located at 3.418 eV and 3.409 eV, respectively. The band edge emission intensity for the GaN on HTAP template is about 9 times higher than that on MGA template. The yellow luminescence band related to defects such as dislocation and impurities that are located at around 2.0-2.6 eV is very weak. In addition, the red-shift of approximately 9 meV for a band edge emission peak was observed. It is known that the band gap energy is affected by the residual stress in a semiconductor thin film[28]. Therefore, this red-shift of the band edge emission peak in the GaN crystal grown on the HTAP template can be attributed to the relief of the compressive stress in GaN crystal and this result is complementary to the result of the Raman measurement. The PL results indicate that the optical quality of the GaN crystal on the HTAP template was improved and the TDs density was decreased.

For the HTAP template, some GaN nucleates selectively at the pores by filling the voids inside the pores. Many voids in the underlying GaN layer are refilled during the early stages of HVPE growth. In this process, bending of dislocations could occur through refilling of the voids. As a result, propagation of dislocations beyond the voids could be suppressed. Some GaN nucleates at the surface and GaN islands of submicrometer size form around the voids. Adjacent GaN islands expand and coalesce forming mesas, and these mesas extend both vertically and laterally on voids, leading eventually to full coalescence. The microscale lateral overgrowth of GaN above voids also contributes to the reduction of dislocations. When facing inclined planes, dislocations are forced to alter orientations by image force[29,30]. Less dislocation will thread to the surface, because lots of dislocations bend to become parallel to the growth face, and annihilate with each other[31]. Some of dislocations in the HTAP template layer may extend into the islands. However, these dislocations toward [0001] is suppressed by the bending of dislocations toward the horizontal direction because of the growth of faceted islands.

Conclusions

In summary, GaN crystals were grown by HVPE on a HTAP template. The HTAP templates with micron-porous structure were fabricated by using the high temperature annealing process under suitable annealed conditions. With this technique numerous voids were generated between the GaN crystal and the HTAP template during the growth. And the voids played an important role in the separation of GaN crystal from HTAP template and the reduction of dislocation density in GaN crystals. The microscale lateral overgrowth of GaN above voids also contributes to the reduction of dislocations. The results demonstrate that the high temperature annealing method is a simple and short procedure to fabricate the HTAP templates, which serve as an excellent template for high-quality GaN film growth.

Acknowledgements

This work was supported by National Basic Research Program of China (2011CB301904), NSFC (Contract 51321091), IIFSDU, China Postdoctoral Science Foundation funded project (2012M521331, 2014T70634), Special Fund from Postdoctoral Innovation Research Program of Shandong Province (201203062).

Notes and references

1 F. A. Ponce and D. P. Bour, *Nature*, 1997, **386**, 351-359.
2 Y. Kobayashi, K. Kumakura, T. Akasaka and T. Makimoto, *Nature*, 2012, **484**, 223–227.
3 K. Chung, C. H. Lee and G. C. Yi, *Science*, 2010, **330**, 655-657.
4 L. S. Yu, Y. Y. Lv, X. L. Zhang, Y. Zhao, Y. L. Zhang, H. Y. Huang and Y. Y. Feng, *CrystEngComm*, 2010, **12**, 2037–2039.
5 K. Kachel, M. Korytov, D. Gogova, Z. Galazka, M. Albrecht, R. Zwierz, D. Siche, S. Golka, A. Kwasniewski, M. Schmidbauer and R. Fornari, *CrystEngComm*, 2012, **14**, 8536–8540.
6 M. G. Mynbaeva, A. E. Nikolaev, A. A. Sitnikova and K. D. Mynbaev, *CrystEngComm*, 2013, **15**, 3640-3646.
7 L. Zhang, Y. L. Shao, X. P. Hao, Y. Z. Wu, S. Qu, X. F. Chen and X. G. Xu, *J. Cryst. Growth*, 2011, **334**, 62-66.
8 Y. Oshima, T. Eri, M. Shibata, H. Sunakawa and A. Usui, *phys. stat. sol. (a)*, 2002, **194**, 554-558.
9 H. H. Huang, C. L. Chao, T. W. Chi, Y. L. Chang, P. C. Liu, L. W. Tu, J. D. Tsay, H. C. Kuo, S. J. Cheng, W. I. Lee, *J. Cryst. Growth*, 2009, **311**, 3029–3032.
10 C. L. Chao, C. H. Chiu, Y. J. Lee, H. C. Kuo, P. C. Liu, J. D. Tsay and S. J. Cheng, *Appl. Phys. Lett.*, 2009, **95**, 051905.
11 H. W. Choi, M. A. Rana, S. J. Chua, T. Osipowicz and J. S. Pan, *Semicond. Sci. Technol.*, 2002, **17**, 1223–1225.
12 M. Kuball, F. Demangeot, J. Frandon, M. A. Renucci, J. Massies, N. Grandjean, R. L. Aulombard and O. Briot, *Appl. Phys. Lett.*, 1998, **73**, 960-962.
13 Y. Tian, L. Zhang, Y. Z. Wu, Y. L. Shao, Y. B. Dai, H. D. Zhang, R. S. Wei, X. P. Hao, *CrystEngComm*, 2014,**16**, 2317-2322.
14 C. D. Yerino, Y. Zhang, B. Leung, M. L. Lee, T. C. Hsu, C. K. Wang, W. C. Han and J. Peng, *Appl. Phys. Lett.* 2011, **98**, 251910.
15 X. Hui, J. Zhang, S. L. Li, H. Wang, Y. Y. Fang, J. N. Dai, C. Q. Chen, *J. Vac. Sci. Technol. B*, 2013, **31**, 050607.
16 B. V. L'vov, *Thermochim. Acta*, 2000, **360**, 85-91.
17 Z. W. Pan, Z. R. Dai, C. Ma, Z. L. Wang, *J. Am. Chem. Soc.* 2002, **124**, 1817-1822.
18 R. C. Schoonmaker, A. Buhl, J. Lemley, *J. Phys. Chem.* 1965, **69**, 3455-3460.
19 G. Jacob, R. Madar and J. Hallais, *Mater. Res. Bull.*, 1976, **11**, 445-450.
20 A. Rebey, T. Boufaden and B. E. Jani, *J. Cryst. Growth*, 1999, **203**, 12-17.
21 A. Bchetnia, I. Kemis, A. Tour´e, W. Fathallah, T. Boufaden and B. E. Jani, Semicond. Sci. Technol. 2008, 23, 125025.
22 A. Pisch and R. Schmid-Fetzer, *J. Cryst. Growth*, 1998, **187**, 329-332.
23 T. S. Oh, Y. S. Lee, H. Jeong, J. D. Kim, T. H. Seo, K. J. Lee, E. K. Suh, *J. Cryst. Growth*, 2009, **311**, 2655–2658.
24 R. Chierchia, T. Bottcher, H. Heinke, S. Einfeldt, S. Figge and D. Hommel, J. Appl. Phys. 2003, 93, 8918.
25 K. Fujito, S. Kubo, I. Fujimura, *MRS Bulletin*, 2009, **34**, 313-317.
26 K. Fujito, S. Kubo, H. Nagaoka, T. Mochizuki, H. Namita, S. Nagao, *J. Cryst. Growth*, 2009, **311**, 3011–3014.
27 S. Tripathy, S. J. Chua, P. Chen and Z. L. Miao, *J. Appl. Phys.*, 2002, **92**, 3503–3510.
28 D. G. Zhao, S. J. Xu, M. H. Xie, S. Y. Tong and H.Yang, *Appl. Phys. Lett.*, 2003, 83, 677.
29 T. S. Zheleva, O. H. Nam, W. M. Ashmawi, J. D. Griffin, R. F. Davis, *J. Cryst. Growth*, 2001, **222**, 706.
30 P. Vennegues, B. Beaumont, V. Bousquet, M. Vaille and P. Gibart, *J. Appl. Phys.*, 2000, **87**, 4175.
31 H. Long, Y. Wei, T. J. Yu, Z. Wang, C. Y. Jia, Z. J.Yang, G. Zhang, S. S. Fan, *CrystEngComm*, 2012,**14**, 4728-4731.